Resilient Expansion Planning of Electricity Grid Under Prolonged Wildfire Risk

Reza Bayani, *Graduate Student Member, IEEE*, and Saeed D. Manshadi, *Member, IEEE*

***Abstract*—Public safety power shut-off (PSPS) during potentially dangerous weather conditions is an emergency measure within areas prone to wildfires. While balancing the risk of wildfire ignition and the continuation of energy supply is a short-term operation challenge, this paper explores the optimal long-term resilient expansion planning strategies. With the quantified risk of wildfire ignition, the proposed expansion planning problem maximizes the supplied power to the end-users while limiting the risk of wildfire ignition. The presented scheme provides utility decision-makers with three groups of network expansion decisions, namely addition of new lines, modification of existing lines, and installation of distributed energy resources (DERs). Given the uncertainty of DERs and wildfire risk, a two-stage robust optimization problem is proposed which ensures power system resilience against unfavorable events. The case studies illustrate how the presented model balances shutting off customers, DER installation, and line addition/modification while inhibiting wildfire ignition risk. Besides, the results suggest that, with appropriate transmission switching, DER installation can be the optimal choice for meeting the growing demand while limiting wildfire ignition risk. The implications of different risk level choices are illustrated, and the impacts of uncertainties on the expansion decisions are explored. Finally, the results of applying the proposed model to the IEEE 118-bus test network are illustrated.**

***Index Terms*—Wildfire, expansion planning, two-stage robust optimization, resilience, uncertainties, natural disasters.**

NOMENCLATURE

Indices and Sets

$b \in \mathcal{B}$	Buses in the power system
$d \in \mathcal{D}$	Electricity demands
$e \in \mathcal{E}$	Set of existing powerlines
$g \in \mathcal{G}$	Generation units
$k \in \mathcal{K}$	Set of iterations (uncertainties) in the algorithm
$l \in \mathcal{L}$	Lines in the power system
$n \in \mathcal{N}$	Set of candidate new lines
$r \in \mathcal{R}$	Renewable generation units
$s \in \mathcal{S}$	Set of periods in the duration curve
$y \in \mathcal{Y}$	Set of planning years
$z \in \mathcal{Z}$	Set of segments in the linearized cost function

Binary Variables

I^N	Decision for construction on new lines
M^E	Decision for modification of existing lines
O^E	Decision for energization status of existing lines
$u^{D/R/\psi}$	Decision for realization of uncertainties in demand, DER energy availability, and wildfire risk
$X^{E/N}$	Auxiliary variable for energization status of modified existing lines or constructed new lines

Continuous Variables

C	Operation cost of the system
$p^{D/G/L/R}$	Real power dispatch of demands, generation units, lines, or DERs
P^R	Installed capacity of DER unit
θ^B	Voltage angle of bus
Ψ^L	Wildfire risk score if line is energized
$\underline{\mu}, \overline{\mu}, \lambda$	Dual variables

Parameters

c^G	Cost of thermal unit generation
$c^{M/N}$	Cost of line modification/ new line addition
H_s	Hours in each period of the duration curve
$\overline{p}^{D/R}$	Forecast demand power and energy availability of DERs
x	Reactance of line
ϕ	Budget of uncertainty (BoU)
κ^D	Unit cost for value of lost load
Λ	An arbitrary large constant
Υ	Wildfire risk tolerance limit of the network
$\Delta^{D/R/\psi}$	Factors for adjusting demand, DER energy availability, and wildfire risk based on uncertainties
$\underline{*}, \overline{*}$	Lower/upper bound value indicators

Manuscript received 6 May 2022; revised 8 October 2022; accepted 10 January 2023. Date of publication 31 January 2023; date of current version 23 August 2023. Paper no. TSG-00652-2022. *(Corresponding author: Saeed D. Manshadi.)*

Reza Bayani is with the Department of Electrical and Computer Engineering, University of California at San Diego, La Jolla, CA 92093 USA, and also with the Department of Electrical and Computer Engineering, San Diego State University, San Diego, CA 92182 USA (e-mail: rbayani@ucsd.edu).

Saeed D. Manshadi is with the Department of Electrical and Computer Engineering, San Diego State University, San Diego, CA 92182 USA (e-mail: smanshadi@sdsu.edu).

Color versions of one or more figures in this article are available at https://doi.org/10.1109/TSG.2023.3241103.

Digital Object Identifier 10.1109/TSG.2023.3241103

I. INTRODUCTION

A. Motivation

IN THE past decades, the number of wildfire events has been following an upward trend [1]. Climate change and higher average temperatures are counted among the contributing factors to this shift [2]. Reportedly, power systems

are listed among the causes of wildfire ignition. From 2015 to 2017, the electricity grid was responsible for 414 wildfire ignitions in California, as declared by Pacific Gas & Electric Company [3]. More than 4,000 wildfires were associated with the electricity grid between 2010 and 2014 in Texas [4]. Compared with other ignition sources, wildfires sparked by power systems are known to be more extensive [5]. Even though only 10% of wildfires are caused by power systems, they are responsible for half of California's catastrophic wildfires [6].

Several factors, including temperature, moisture, precipitation, elevation, slope, and vegetation (age, composition, and distribution), contribute to wildfire intensity and extent within electricity grids [7]. However, these elements are almost irrelevant in the first place, as wildfire ignition by power systems is strongly correlated with wind conditions. It is known that the probability of failures within the electricity grid increases dramatically with the rise in wind speed and gust [8]. Vegetation-driven ignitions caused by electric arcs, phase-to-ground faults, clashing of neighboring conductors (phase-to-phase faults), and contact of powerlines with the surrounding plants are recognized as major wildfire ignition causes by power systems [9]. Wind could lead to wildfire ignition in power systems either directly or indirectly. In conductor clashing (a.k.a. line slap), wind directly causes powerline conductors to contact each other, potentially releasing hot molten particles that could ignite the combustible material below. Wind also indirectly causes surrounding trees and branches to break powerlines and lead to phase-to-ground faults [10].

Appropriate risk assessment tools are critical to the operation of power systems facing wildfire outbursts. To this end, forest fire danger index (FFDI), Keetch–Byram drought index, fire potential index (FPI), and Forest Fire Ignition Probability Map are among the forecast tools that are widely used worldwide. The resulting situational awareness information is then utilized to decide on various preventive exercises such as line de-energization, network topology control, redispatch of generation units, and load shedding [11]. In order to prevent wildfire ignition, utilities in California embrace *public safety power shut-off* (PSPS) events during extreme wind conditions by forcing mandatory outages on end-users. During the period from 2019 to 2021, California utilities have conducted 70 PSPS events [6]. Based on short-term weather forecasts, utilities perform shut-offs when wind speeds or gusts are estimated to reach exceedingly hazardous levels.

In practice, performing PSPSs is extremely costly for both the utility and the impacted communities; that is why they are deemed the last resort. PSPS events last an average of two days, and the impacted families who cannot afford backup generation should either evacuate, engage in emergency power plans, or prepare to live without power for 2-6 days [12]. PSPS events are particularly harmful to low-income communities and medically vulnerable populations [13]. Some estimates suggest that PSPS events cost the California economy in the order of billions of dollars [14]. From the utility viewpoint, besides the loss of revenues, scheduling a PSPS will induce a variety of operational costs including but not limited to data acquisition and situational awareness tools, switching (installation, sectionalizing, and maintenance), consumer interactions (providing temporary generation and storage devices, communications, legal, etc.), and restoration. Here, the value of lost load (VOLL) is utilized as a surrogate for the utility costs of line de-energizing under wildfire risk.

A pre-planned operation is essential to ensure the power system's reliability in providing energy to the customers. The primary purpose of expansion planning is to make certain the power grid can keep up with system-wide changes such as electricity demand growth, changes in the generation fleet portfolio, or even climate change, which could potentially impact the system's operations over the long term. The main goal of this paper is to present an expansion planning model that takes wildfire ignition risk associated with power systems into consideration. PSPS events are not included in the long-term planning, which motivated us to propose a model that integrates the impacts of scheduled shut-offs into expansion planning. With the looming threat of disastrous wildfires, the proposed resilient expansion planning model mitigates the overall wildfire risk of a power system and minimizes the consequences of PSPS events for both the utility and the customers.

In our previous work, we presented a risk score that quantifies the risk of wildfire ignition caused by conductor clashing [15]. It should be noted that surrounding vegetation fuel is the determining factor in wildfire spread [16]. In addition to that, wildfire ignition is also dependent on other factors such as wind, humidity, and temperature. It is assumed that a similar scoring metric is available that incorporates all of the factors that impact wildfire ignitions within a power grid. The term *wildfire risk score* in this work essentially represents the likelihood (hence a parameter between 0 and 1) of ignitions. A duration curve is generated which segregates each year into several periods attributed to distinct values of demand, renewable generation available energy, and wildfire ignition risk. Since these values are not deterministic and can be affected by stochasticities, a robust solution method is proposed that accounts for these uncertainties.

The proposed wildfire-resilient framework provides system planners with a planning tool that accounts for wildfire hazardous conditions that necessitate power shut-offs. The presented model aims to find the optimal expansion decisions considering the risk of wildfires, a crucial aspect that is non-existent in the relevant literature. The network expansion decisions in this work are categorized into three groups: addition of new lines, modification of the existing lines (i.e., hardening measures), and installation of distributed energy resources (DERs). In this work, modification denotes hardening measures that make power lines less vulnerable to conditions that induce ignitions. For example, Californian utilities such as San Diego Gas & Electric and Southern California Edison have adopted the practice of covering bare conductors (a.k.a. reconductoring) to mitigate ignition probability through contact with neighboring wires, objects, and structures such as cross arms [17], [18]. Other modification practices in power systems include burying lines (a.k.a. undergrounding), relocation of a line to an area with a lower wildfire ignition risk, anchoring, increasing

the number of poles/towers, replacing wood poles with steel, installing high-strength conductors, and increasing conductor spacing [11]. In our proposed model, line modification is among the planning decisions that the decision-maker takes to reduce the wildfire risk of a line at a cost.

B. Literature Review

The power system expansion planning problem has been thoroughly investigated from various standpoints, such as transmission expansion [19], distribution expansion [20], generation expansion [21], microgrid expansion [22], and simultaneous generation and transmission expansion [23]. In addition, with the rapidly increasing interest in renewable generation, expansion planning of power systems subject to the growing penetration of these resources has grabbed research attention [24]. Apart from expansion planning to match the growing demand and renewable integration, researchers have also studied the expansion problem considering environmental conditions, such as climate change scenarios [25] and rising temperatures [26]. In all of the mentioned aspects of the expansion planning problem, the model parameters can be considered deterministic [27] or stochastic [28]. Common approaches for tackling uncertainties in these problems include but are not limited to scenario-based methods [29], chance-constrained models [30], and multi-stage approaches relying on feasibility/optimality cuts such as column and constraint generation algorithm [31] and Benders decomposition [32].

Expansion planning with the aim of improving power network resilience against natural disasters has been a subject of interest. Optimal DER and switch placement considering extreme weather scenarios are investigated in [33]. A model for transmission network upgrade to improve resilience against natural disasters is discussed in [34]. An integrated electricity-natural gas system expansion planning model to enhance the resilience of the electricity grid against natural disasters is presented in [35]. A two-stage robust optimization and co-expansion planning problem in integrated gas and power systems to increase resilience against natural disasters is presented in [36]. A generation and transmission expansion planning to increase the resilience of the power system against earthquakes and floods is presented in [37]. However, none of the works in the literature investigates the expansion planning problem considering wildfire risk. The need for a resilient long-term planning framework to hedge against disastrous wildfires has been highlighted in [11].

Most recently, the increasing occurrences of wildfires have attracted research focus on this issue. Distribution grid resilience in the case of ongoing wildfires considering uncertainties in wildfire progression is discussed in [38]. The resilient operation of a transmission network in case of stochastic wildfires is investigated in [39] with an attacker-defender approach. Improving grid resilience during wildfires by means of electric vehicles is also studied [40]. An overview of the wildfire mitigation plans in power systems is presented in [41]. According to the authors of [41], the existing literature treats wildfires the same as other natural disasters, while the interactions between the power system and wildfires are unique (as power systems can contribute to the ignition of wildfires). This work fills the mentioned gaps in the literature by proposing a wildfire-resilient expansion planning problem. The scheduled power shut-offs as a response to wildfire risk are modeled, and the quantified wildfire risk is considered.

C. Summary of the Contributions

The main contributions of this paper are outlined as follows:

1) A framework for wildfire-resilient expansion planning is presented for electricity grids under prolonged risk of wildfire ignition. An advantage of the proposed method is that it can incorporate any given wildfire risk assessment metric. Based on the risk scores associated with each line, the objective is to establish a balance between preemptive de-energization of powerlines and expansion planning decisions, including addition of new lines, modification of existing lines, and installation of DER units.
2) The introduced model enables system planners with two control parameters, namely risk tolerance (Υ) and budget of uncertainty (BoU) (Φ). The former inhibits the overall wildfire ignition risk induced by the power system, while the latter is determined by the planner's willingness to take risks.
3) A two-stage solution method is utilized to ensure planning robustness against uncertainties not only in terms of system demand and DER energy availability but also wildfire risk. The proposed algorithm iteratively seeks worse-case uncertainties based on planning decisions obtained in the wildfire-resilient step. The resilient operation of the network is established once the realized uncertainties cannot further aggravate the system's operation.
4) The effects of the planner's desired risk tolerance level are explored as a major driver impacting the decisions. Besides, several cases are presented that investigate and analyze the impacts of uncertainties and transmission switching on the expansion decisions of the network.

II. Problem Formulation

The wildfire-resilient expansion planning problem is formulated as a two-stage robust optimization problem that accounts for uncertainties in the system demand as well as DER energy availability and wildfire risk. The first-stage problem minimizes the overall costs of the system, including expansion costs and operation costs. The *here-and-now* decision variables P, I, and M are retrieved and then passed to the second stage. The second-stage problem is a *wait-and-see* step at which the uncertainties in system demand, DER generation, and wildfire risk are determined. In this step, we are interested in finding a subset of worst-case uncertainties for the current *here-and-now* decisions given a budget of uncertainty as part of a robust optimization approach. In an iterative process, a new subset of uncertainty realizations is obtained at the second-stage problem and added to the uncertainty set $\mathcal{K}$, which is passed back to the first-stage problem to update *here-and-now* decisions. The uncertain parameters are realized according to

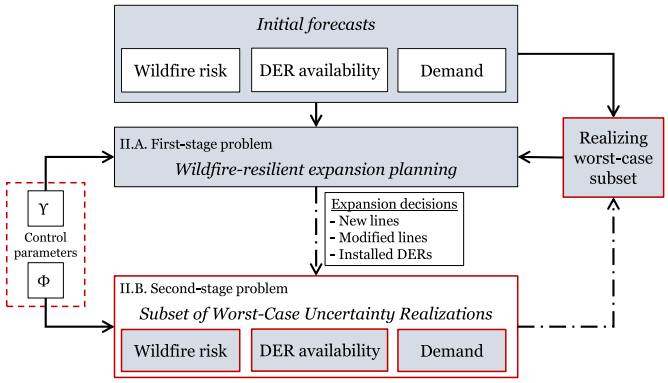

Fig. 1. The flow diagram of the proposed modeling approach.

their deviation factor Δ from the deterministic values. This procedure repeats until the expansion planning decisions are no longer updated, i.e., worst-case realizations are determined. The diagram of the proposed model is presented in Fig. 1.

A. Wildfire-Resilient Expansion Planning

The problem formulation for obtaining the *here-and-now* decisions of the wildfire-resilient expansion planning problem is presented in (1). The objective function is comprised of two parts. The first part accounts for the expansion costs of the system, composed of the costs of new line construction, DER installation, and line modification, respectively represented by the first three terms in (1a). The second part of the objective function represents the operation costs of the system over the planning horizon, given by (1b). This term includes the monetized load shedding penalty and the cost of electricity generation, represented by the first and second terms in (1b), respectively. The cost parameters are indexed by 'y' to incorporate the inflation rates. If the scheduled PSPS events lead to the discontinuation of energy supply, they will be penalized through this approach. After each iteration of the proposed algorithm, a new set of *wait-and-see* decisions is obtained, which leads to different operation costs. According to (1b), the operation cost of the system is considered the highest one among all of the realized uncertainty subsets.

$$\min_{P,I,M} \sum_{\mathcal{Y}} \left\{ \begin{array}{l} +\sum_{\mathcal{N}} c^N_{l,y}\left(I^N_{l,y} - I^N_{l,y-1}\right) \\ +\sum_{\mathcal{R}} c^R_{r,y}\left(P^R_{r,y} - P^R_{r,y-1}\right) \\ +\sum_{\mathcal{E}} c^M_{l,y}\left(M^E_{l,y} - M^E_{l,y-1}\right) \end{array} \right\} + C \tag{1a}$$

subject to:

$$C \geq \sum_{\mathcal{Y}} \sum_{\mathcal{S}} H_s \left\{ \begin{array}{l} \sum_{\mathcal{D}} \kappa^D \left(\overline{p}^{D,k}_{d,s,y} - p^{D,k}_{d,s,y}\right) \\ +\sum_{\mathcal{G}} \sum_{\mathcal{Z}} c^G_{g,z} \cdot p^{G,k}_{g,z,s,y} \end{array} \right\}, \quad \forall\, \mathcal{K} \tag{1b}$$

$$\underline{p}^G_g \leq p^{G,k}_{g,s,y} \leq \overline{p}^G_g, \quad \forall\, \mathcal{G}, \mathcal{S}, \mathcal{Y}, \mathcal{K} : \underline{\mu}^G_{g,s,y}, \overline{\mu}^G_{g,s,y} \tag{1c}$$

$$0 \leq p^{G,k}_{g,z,s,y} \leq \overline{p}^G_{g,z}, \quad \forall\, \mathcal{G}, \mathcal{Z}, \mathcal{S}, \mathcal{Y}, \mathcal{K} : \overline{\mu}^G_{g,z,s,y} \tag{1d}$$

$$\sum_{\mathcal{Z}} p^{G,k}_{g,z,s,y} = p^{G,k}_{g,s,y}, \quad \forall\, \mathcal{G}, \mathcal{S}, \mathcal{Y}, \mathcal{K} : \lambda^G_{g,s,y} \tag{1e}$$

$$\underline{\theta}^B_b \leq \theta^{B,k}_{b,s,y} \leq \overline{\theta}^B_b, \quad \forall\, \mathcal{B}, \mathcal{S}, \mathcal{Y}, \mathcal{K} : \underline{\mu}^\theta_{b,s,y}, \overline{\mu}^\theta_{b,s,y} \tag{1f}$$

$$0 \leq p^{R,k}_{r,s,y} \leq P^R_{r,y} \cdot \overline{p}^{R,k}_{r,s,y}, \quad \forall\, \mathcal{R}, \mathcal{S}, \mathcal{Y}, \mathcal{K} : \overline{\mu}^R_{r,s,y} \tag{1g}$$

$$0 \leq p^{D,k}_{d,s,y} \leq \overline{p}^{D,k}_{d,s,y}, \quad \forall\, \mathcal{D}, \mathcal{S}, \mathcal{Y}, \mathcal{K} : \overline{\mu}^D_{d,s,y} \tag{1h}$$

$$\sum_{G_b} p^{G,k}_{g,s,y} + \sum_{R_b} p^{R,k}_{r,s,y} + \sum_{\mathcal{L}^{to}_b} p^{L,k}_{l,s,y} - \sum_{\mathcal{L}^{fr}_b} p^{L,k}_{l,s,y} = \sum_{D_b} p^{D,k}_{d,s,y}, \quad \forall\, \mathcal{B}, \mathcal{S}, \mathcal{Y}, \mathcal{K} : \lambda^B_{b,s,y} \tag{1i}$$

$$-\Lambda\left(1 - O^E_{l,s,y} - X^N_{l,s,y}\right) + p^{L,k}_{l,s,y} \leq \frac{\theta^{B,k}_{b^{fr}_l,s,y} - \theta^{B,k}_{b^{to}_l,s,y}}{x_l} \leq \Lambda\left(1 - O^E_{l,s,y} - X^N_{l,s,y}\right) + p^{L,k}_{l,s,y}, \quad \forall\, \mathcal{L}, \mathcal{S}, \mathcal{Y}, \mathcal{K} : \underline{\mu}^O_{l,s,y}, \overline{\mu}^O_{l,s,y} \tag{1j}$$

$$-\overline{p}^L_l\left(O^E_{l,s,y} + X^N_{l,s,y}\right) \leq p^{L,k}_{l,s,y} \leq \overline{p}^L_l\left(O^E_{l,s,y} + X^N_{l,s,y}\right), \quad \forall\, \mathcal{L}, \mathcal{S}, \mathcal{Y}, \mathcal{K} : \underline{\mu}^L_{l,s,y}, \overline{\mu}^L_{l,s,y} \tag{1k}$$

$$\Psi^{L,k}_{l,s,y} = \psi^{L,k}_{l,s,y}\left(O^E_{l,s,y} + X^N_{l,s,y} - \alpha^\psi \cdot X^E_{l,s,y}\right), \quad \forall\, \mathcal{L}, \mathcal{S}, \mathcal{Y}, \mathcal{K} \tag{1l}$$

$$\sum_{\mathcal{L}} \sum_{\mathcal{S}} H_s \cdot \Psi^{L,k}_{l,s,y} \leq \Upsilon, \quad \forall\, \mathcal{Y}, \mathcal{K} \tag{1m}$$

$$X^E_{l,s,y} \leq M^E_{l,y}, \quad \forall\, \mathcal{E}, \mathcal{S}, \mathcal{Y} \tag{1n}$$

$$X^E_{l,s,y} \leq O^E_{l,s,y}, \quad \forall\, \mathcal{E}, \mathcal{S}, \mathcal{Y} \tag{1o}$$

$$X^E_{l,s,y} \geq M^E_{l,y} + O^E_{l,s,y} - 1, \quad \forall\, \mathcal{E}, \mathcal{S}, \mathcal{Y} \tag{1p}$$

$$I^N_{l,y} \geq I^N_{l,y-1}, \quad \forall\, \mathcal{N}, \mathcal{Y} \tag{1q}$$

$$M^E_{l,y} \geq M^E_{l,y-1}, \quad \forall\, \mathcal{E}, \mathcal{Y} \tag{1r}$$

$$P^R_{r,y} \geq P^R_{r,y-1}, \quad \forall\, \mathcal{R}, \mathcal{Y} \tag{1s}$$

The real power outputs of generation units are bounded by (1c). The generation cost of the thermal units is approximated by a piecewise linear function, where the power of each segment is limited by (1d). The dispatched power of each generation unit is equal to the summation of its segmented powers, as constrained by (1e). The voltage angle on each bus is bounded by (1f). The dispatched power of DER units is constrained by (1g) where $\overline{p}^R$ is a parameter ranging from 0 to 1 and represents the amount of renewable resource energy availability at each period in the duration curve. Since there is no distinction between governing equations of different renewable units (i.e., wind and solar DERs), they are modeled under the same set. The served demand power is limited by (1h) where $\overline{p}^D$ is a parameter representing the demand at each period in the duration curve. The nodal balance at each bus is given by (1i). The power flow equation is based on DC approximation and is modeled by (1j). These inequality constraints turn into an equality equation if a pre-existing line (O^E) or a newly constructed line (X^N) is energized, in which case the expression $(1 - O^E_{l,s,y} - X^N_{l,s,y})$ becomes 0. A similar logic is utilized in (1k) to enforce the thermal limit of power flowing through energized lines. This time, the real power flowing through the line is always 0 unless the line is energized, in which case the thermal constraints are applied.

The wildfire risk score of each line is calculated according to (1l). To obtain the quantified wildfire risk score ψ, it is supposed that the metric used in our previous work [15] can be extended to integrate all factors that affect wildfire ignition risk including but not limited to wind speed, vegetation, and humidity. The proposed expansion method is not limited to

the choice of wildfire risk indicator and can adapt to indices such as FPI and FFDI. For all energized lines, Ψ equals the quantified risk score of that line. If a line is modified, its score is adjusted by α^{ψ} which is a parameter between 0 and 1. To prevent wildfire-hazardous operation, the total wildfire risk of the system in each year is limited to the risk tolerance Υ according to (1m). This score is calculated by physically modeling the 3D non-linear vibrational motion of powerlines which considers numerous physical, structural, and meteorological features including but not limited to the span of the powerline, conductor diameter, and wind speed. Equations (1n), (1o), and (1p) are used to maintain the linearity of the problem. These equations are equivalent to the binary formulation $X^E = M^E \cdot O^E$. The same linear transformation is utilized to enforce the formulation $X^N = I^N \cdot O^N$. In the end, Eqs. (1q), (1r), and (1s) are utilized to keep track of the planning decisions made in previous years. In front of each constraint in (1), the corresponding dual variables are displayed. It is noticed that in the proposed expansion planning formulation, the parameters $\overline{p}^{D,k}_{d,s,y}$, $\overline{p}^{R,k}_{r,s,y}$, and $\psi^{L,k}_{l,s,y}$ are indexed by k. These parameters denote the realized uncertainties based on the results of the second-stage problem.

B. Subset of Worst-Case Uncertainty Realizations

In this part, two formulations are proposed which respectively find the worst-case uncertainty realizations for variations in DER generation, demand power, and wildfire risk.

1) Uncertainties in DER Generation and Electricity Demand: The dual formulation by which the worst-case realizations in DER energy availability and demand are obtained is presented in (2). The dual objective is given by (2a) and the dual constraints are described in (2b) through (2i). In front of each dual constraint, the corresponding primal variables are displayed. The goal of the presented problem is to find the binary decisions u that lead to the worst-case realizations. In order to obtain the *wait-and-see* decisions, the objective function (2a) should be maximized. According to the proposed model, if uncertainties are realized in demand or DER energy availability, their corresponding values are adjusted by Δ. Since we are only interested in the worst-case realizations, it is supposed that the uncertainties only increase the demand and reduce the DER energy availability. The total count of realized uncertainties is enforced by the BoU as given in (2h). The hat sign on top of *here-and-now* decision variables in the dual objective denotes that these variables are passed from the first-stage problem.

$$\max_{u,\mu,\lambda} \sum_{\mathcal{S}} \sum_{\mathcal{Y}} \left\{ \begin{array}{c} -\sum_{\mathcal{G}} \sum_{\mathcal{Z}} \overline{p}^{G}_{g,z} \cdot \overline{\mu}^{G}_{g,z,s,y} \\ +\sum_{\mathcal{G}} \left(\underline{p}^{G}_{g} \cdot \underline{\mu}^{G}_{g,s,y} - \overline{p}^{G}_{g} \cdot \overline{\mu}^{G}_{g,s,y} \right) \\ +\sum_{\mathcal{B}} \left(\underline{\theta}^{B}_{b} \cdot \underline{\mu}^{\theta}_{b,s,y} - \overline{\theta}^{B}_{b} \cdot \overline{\mu}^{\theta}_{b,s,y} \right) \\ +\sum_{\mathcal{D}} \kappa^{D} \cdot \overline{p}^{D,k}_{d,s,y} \left(1 + \Delta^{D} \cdot u^{D}_{d,s,y} \right) \\ -\sum_{\mathcal{D}} \overline{p}^{D,k}_{d,s,y} \cdot \overline{\mu}^{D}_{d,s,y} \left(1 + \Delta^{D} \cdot u^{D}_{d,s,y} \right) \\ -\sum_{\mathcal{R}} \hat{P}^{R}_{r,y} \cdot \overline{p}^{R,k}_{r,s,y} \cdot \overline{\mu}^{R}_{r,s,y} \left(1 - \Delta^{R} \cdot u^{R}_{r,s,y} \right) \\ -\sum_{\mathcal{L}} \Lambda \left(1 - \hat{O}^{E}_{l,s,y} - \hat{X}^{N}_{l,s,y} \right) \left(\underline{\mu}^{O}_{l,s,y} + \overline{\mu}^{O}_{l,s,y} \right) \\ -\sum_{\mathcal{L}} \overline{p}^{L}_{l} \left(\hat{O}^{E}_{l,s,y} + \hat{X}^{N}_{l,s,y} \right) \left(\underline{\mu}^{L}_{l,s,y} + \overline{\mu}^{L}_{l,s,y} \right) \end{array} \right\} \tag{2a}$$

subject to:

$$\underline{\mu}^{G}_{g,s,y} - \overline{\mu}^{G}_{g,s,y} - \lambda^{G}_{g,s,y} + \sum_{B_g} \lambda^{B}_{b,s,y} = 0, \quad \forall\, \mathcal{G}, \mathcal{S}, \mathcal{Y} : p^{G}_{g,s,y} \tag{2b}$$

$$-\overline{\mu}^{G}_{g,z,s,y} + \lambda^{G}_{g,s,y} \le H_s \cdot c^{G}_{g,z}, \quad \forall\, \mathcal{G}, \mathcal{Z}, \mathcal{S}, \mathcal{Y} : p^{G}_{g,z,s,y} \tag{2c}$$

$$-\overline{\mu}^{D}_{d,s,y} - \sum_{\mathcal{B}_d} \lambda^{B}_{b,s,y} \le -H_s \cdot \kappa^{D}, \quad \forall\, \mathcal{D}, \mathcal{S}, \mathcal{Y} : p^{D}_{d,s,y} \tag{2d}$$

$$-\overline{\mu}^{R}_{r,s,y} + \sum_{\mathcal{B}_r} \lambda^{B}_{b,s,y} \le 0, \quad \forall\, \mathcal{R}, \mathcal{S}, \mathcal{Y} : p^{R}_{r,s,y} \tag{2e}$$

$$\underline{\mu}^{\theta}_{b,s,y} - \overline{\mu}^{\theta}_{b,s,y} + \sum_{\mathcal{L}^{to}_b} \frac{\underline{\mu}^{O}_{l,s,y} - \overline{\mu}^{O}_{l,s,y}}{x_l} - \sum_{\mathcal{L}^{fr}_b} \frac{\underline{\mu}^{O}_{l,s,y} - \overline{\mu}^{O}_{l,s,y}}{x_l} = 0, \quad \forall\, \mathcal{B}, \mathcal{S}, \mathcal{Y} : \theta^{B}_{b,s,y} \tag{2f}$$

$$\underline{\mu}^{L}_{l,s,y} - \overline{\mu}^{L}_{l,s,y} + \underline{\mu}^{O}_{l,s,y} - \overline{\mu}^{O}_{l,s,y} + \sum_{\mathcal{B}^{fr}_l} \lambda^{B}_{b,s,y} - \sum_{\mathcal{B}^{to}_l} \lambda^{B}_{b,s,y} = 0, \quad \forall\, \mathcal{L}, \mathcal{S}, \mathcal{Y} : p^{L}_{l,s,y} \tag{2g}$$

$$\sum_{\mathcal{S}} \sum_{\mathcal{Y}} \left(\sum_{\mathcal{R}} u^{R}_{r,s,y} + \sum_{\mathcal{D}} u^{D}_{d,s,y} \right) \le \phi, \tag{2h}$$

$$\overline{\mu}, \underline{\mu} \ge 0, \lambda \tag{2i}$$

It is noticed that in the objective function of the dual problem, some non-linear terms appear that contain binary-to-continuous variable multiplication. To avoid solving a non-linear problem of this kind, a linearization process is applied which is exemplified in (3). Here, the non-linear term in (3a) is linearized by (3b)-(3d), where $u^{R}_{r,s,y}$ is a binary variable. Two auxiliary positive continuous variables ν and ω which are bounded between 0 and Λ are required for this linearization procedure.

$$\nu^{R}_{r,s,y} = \overline{\mu}^{R}_{r,s,y} \cdot u^{R}_{r,s,y}, \quad \forall\, \mathcal{R}, \mathcal{S}, \mathcal{Y} \tag{3a}$$

$$\nu^{R}_{r,s,y} = \overline{\mu}^{R}_{r,s,y} - \omega^{R}_{r,s,y}, \quad \forall\, \mathcal{R}, \mathcal{S}, \mathcal{Y} \tag{3b}$$

$$0 \le \nu^{R}_{r,s,y} \le \Lambda \cdot u^{R}_{r,s,y}, \quad \forall\, \mathcal{R}, \mathcal{S}, \mathcal{Y} \tag{3c}$$

$$0 \le \omega^{R}_{r,s,y} \le \Lambda \cdot \left(1 - u^{R}_{r,s,y} \right), \quad \forall\, \mathcal{R}, \mathcal{S}, \mathcal{Y} \tag{3d}$$

The same procedure is also applied to linearize the bi-linear term $\nu^{D}_{r,s,y} = \overline{\mu}^{D}_{r,s,y} \cdot u^{D}_{r,s,y}$.

2) Uncertainties in Wildfire Risk: In this part, a formulation is presented in (4) which realizes the worst-case uncertainties in the wildfire risk scores, which can be raised by factors such as variations in weather conditions. The objective function (4a) aims to find the subset of binary decisions that maximize the overall wildfire risk score of the network. It is supposed that the worst-case realizations will only intensify the wildfire ignition risk, i.e., the parameter ψ is increased by Δ^{ψ}. According to (4b), only the energized lines may be subject to deviations in the wildfire risk. Additionally, the total number of realized uncertainties cannot exceed the allocated budget as enforced

Algorithm 1: Robust Wildfire-Resilient Expansion Planning

Input : $\epsilon,\ \phi,\ \phi^{\psi},\ \Upsilon$
Output: $\hat{P},\ \hat{I},\ \hat{M}$
Initiate: $\hat{k} \leftarrow 1,\ \chi_{(0)} \leftarrow 0,\ \eta \leftarrow 100$
1 **while** $\eta \geq \epsilon$ **do**
2 $\quad \mathcal{K} \leftarrow \{1 : \hat{k}\}$
3 $\quad \chi_{(\hat{k})} \leftarrow$ value of (1a)
4 $\quad \hat{P},\ \hat{I},\ \hat{M} \leftarrow$ (1)
5 $\quad \eta \leftarrow \dfrac{\chi_{(\hat{k})} - \chi_{(\hat{k}-1)}}{\chi_{(\hat{k}-1)}} \times 100$
6 $\quad \hat{u}^{R},\ \hat{u}^{D} \leftarrow$ (2)
7 $\quad \hat{u}^{\psi} \leftarrow$ (4)
8 $\quad \overline{p}^{D,\hat{k}+1}_{d,s,y} = \overline{p}^{D,\mathbf{1}}_{d,s,y}(1 + \Delta^{D} \cdot \hat{u}^{D}_{d,s,y}), \qquad \forall\, \mathcal{D}, \mathcal{S}, \mathcal{Y}$
9 $\quad \overline{p}^{R,\hat{k}+1}_{r,s,y} = \overline{p}^{R,\mathbf{1}}_{r,s,y}(1 - \Delta^{R} \cdot \hat{u}^{R}_{r,s,y}), \qquad \forall\, \mathcal{R}, \mathcal{S}, \mathcal{Y}$
10 $\quad \psi^{L,\hat{k}+1}_{l,s,y} = \psi^{L,\mathbf{1}}_{l,s,y}(1 + \Delta^{\psi} \cdot \hat{u}^{\psi}_{l,s,y}), \qquad \forall\, \mathcal{L}, \mathcal{S}, \mathcal{Y}$
11 $\quad \hat{k} \leftarrow \hat{k} + 1$
12 **end**

by (4c).

$$\max_{u} \sum_{\mathcal{L}} \sum_{\mathcal{S}} \sum_{\mathcal{Y}} H_s \cdot \Psi^{L,k}_{l,s,y} \left(1 + \Delta^{\psi} \cdot u^{\psi}_{l,s,y}\right) \tag{4a}$$

$$u^{\psi}_{l,s,y} \leq \hat{O}^{E}_{l,s,y} + \hat{X}^{N}_{l,s,y}, \quad \forall\, \mathcal{L}, \mathcal{S}, \mathcal{Y} \tag{4b}$$

$$\sum_{\mathcal{L}} \sum_{\mathcal{S}} \sum_{\mathcal{Y}} u^{\psi}_{l,s,y} \leq \phi^{\psi}, \tag{4c}$$

III. Solution Methodology

The steps for solving the wildfire-resilient expansion planning problem are presented in Alg. 1. The convergence threshold, BoU, and risk tolerance are the inputs, while the installed capacity of the DER resources and the decisions for the construction and modification of lines are the outputs of this algorithm. In the initial step, the current realization ($\hat{k}$) is set, and the convergence indicator (η) is assigned an arbitrarily large value. The algorithm's convergence is determined based on a relative iterative error of χ, which represents the overall system planning and operation costs, i.e., the objective value of (1). At the beginning of each iteration, the convergence criteria are checked. Steps 2-11 of Alg. 1 are repeated until the convergence indicator drops below ϵ, in which case the solution process culminates and the latest expansion decisions are reported as the final solution.

In lines 3 and 4, the wildfire-resilient expansion planning problem (1) is solved, and its objective value is assigned to the upper-bound variable χ. As a result, the *here-and-now* decisions that indicate the DER installed capacity and line construction/modification are obtained and stored. In line 5, the convergence indicator is calculated as the relative difference of consecutive planning costs. Next, the worst-case uncertainty realizations are found according to the results of the expansion stage. To find the binary decision variables that cause the worst-case realizations in demand and DER energy availability, problem (2) is solved in line 6. Similarly, in line 7, problem (4) is solved to find the worst-case realizations in wildfire risk. Finally, in lines 8-10, the binary decisions obtained in lines 6 and 7 are used to update the demand, DER energy availability, and wildfire risk values utilized for the next iteration of the algorithm. In line 11, the current set of uncertainties is updated to include the latest worst-case scenarios. Steps 2-11 are placed in a *while* loop, meaning they are repeated until the convergence condition is satisfied, in which case the expansion planning decisions returned at the last iteration are reported as the solution. System decision-makers can utilize Alg. 1 according to their wildfire risk tolerance level and obtain wildfire-resilient expansion decisions.

TABLE I
Demand, DER Energy Availability, and Duration of Each Period

Period	Hour	Season	Demand	Wind	Solar Insolation	Duration (hours)
1	21 - 6	Summer	low	very low	none	1,647
2	6 - 16	Summer	high	very low	high	1,830
3	16 - 21	Summer	very high	very low	medium	915
4	21 - 24	Winter	low	high	none	546
5	24 - 6	Winter	low	medium	none	1,092
6	6 - 16	Winter	medium	low	medium	1,820
7	16 - 21	Winter	high	very low	none	910

IV. Results and Discussions

In this section, several case studies are presented to investigate the effectiveness of the proposed wildfire-resilient expansion planning problem for a 10-year planning horizon. First, the results of applying the robust expansion planning algorithm to a 6-bus system are illustrated. To demonstrate the merits of including wildfire risk tolerance and uncertainties in the proposed wildfire-resilient expansion model, two subsections are presented in Sections IV-A1 and IV-A2, respectively. In the next case, an analysis of the impact of wildfire risk tolerance level on the planner's decision-making process is presented. This case is followed by a part entirely devoted to discussing the effects of transmission switching. Additionally, a sensitivity analysis is provided to illustrate how different BoUs affect the planning decisions. A case is also presented to discuss the impact of candidate line choice on expansion planning decisions and costs. This section is culminated by illustrating the performance of the algorithm on the IEEE 118-bus system to demonstrate model scalability. According to Table I, 7 periods are considered in the duration curve, which correspond to different demands, DER energy availability levels, and wildfire risk scores. To reflect the varying nature of DER generation due to weather fluctuations, the energy availability of DERs changes from year to year.

In practice, transmission line routing is a complicated process and involves trade-offs among a myriad of factors including environmental, political, and social considerations, permitting, right of way acquisition, project need, constructability, current and future identified land use, project

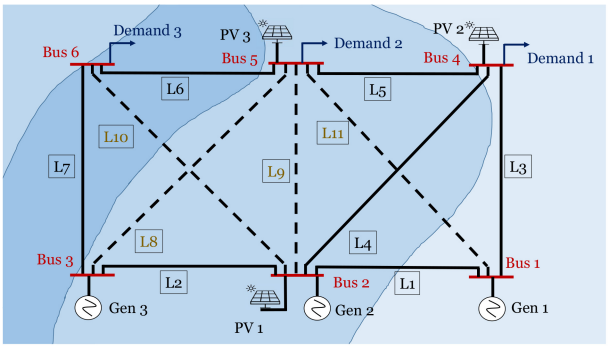

Fig. 2. Schematic of the test 6-bus system.

TABLE II
BASE VALUES FOR RISK SCORE AND DEMAND IN THE 6-BUS NETWORK

Year	$\psi^L_{l_3,s_2,y}$	$\psi^L_{l_3,s_4,y}$	$\psi^L_{l_7,s_2,y}$	$\psi^L_{l_7,s_4,y}$	Demand (GWh)
1	0.0003	0.0028	0.0059	0.0592	3,652.0
4	0.0003	0.0030	0.0064	0.0639	3,875.6
7	0.0003	0.0026	0.0054	0.0510	4,112.9
10	0.0003	0.0027	0.0056	0.0558	4,364.5

costs, and specific electric grid limitations and opportunities [42]. The location and construction cost of each new transmission line is dependent on its specific set of conditions in real-world applications. However, without the loss of generality and in order to showcase the performance of our presented framework, the construction cost of new lines is assumed to be $500,000 per mile and the modification cost of existing lines is considered $250,000 per mile. In all of our experiments, the parameter α^{ψ} is set to 0.5, meaning the wildfire ignition risk is reduced by half once a line is modified.

A. Demonstration of the Proposed Planning Problem

This part illustrates the results of applying the wildfire-resilient planning algorithm to the 6-bus transmission network displayed in Fig. 2. This system includes 3 thermal units, 3 candidate DER installation sites, and 7 powerlines, where candidate lines are distinguished by dashed lines. In experiments of this part, only L_8 and L_9 are included in the set of candidate lines. In part E, a case is presented that includes all lines L_8, L_9, L_{10}, and L_{11} in the set of candidate lines. The shaded areas in the network symbolize different wind speeds throughout the network, with darker shades representing regions prone to higher wind speeds. In this case, the risk tolerance is set to 0.02 and the BoU is set to 15%. It is also assumed that the network's overall demand grows by 2% each year.

The base values for wildfire risk score of select lines and periods along with the overall demand at select years in the planning horizon for this network are shown in Table II. These numbers represent only the predicted values and are subject to change due to the realization of uncertainties. In the first column of this table, the planning years are displayed, and the second and third columns, respectively, show the wildfire risk score associated with line '3' of the network at periods 2 and 4 of the duration curve. The second period is associated with low wind speeds, while period 4 represents high wind speed conditions. The wildfire risk scores for line '7' at the same periods are displayed in the next two columns. As the risk values suggest, since line '7' is placed in a high-wind region, its risk scores are considerably higher than those associated with line '3', which is located in a low-wind region. Finally, the total demand in each year is shown in the last column of this table.

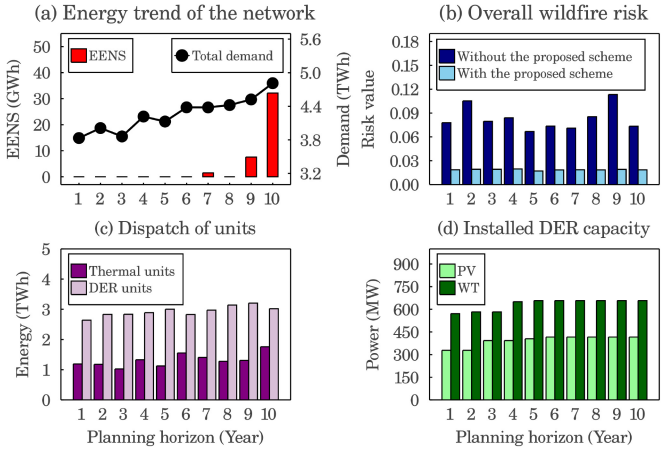

Fig. 3. Expansion planning decisions in the 6-bus network.

According to the planning results, this network requires the addition of two new lines (lines 8 and 9, in year 1), while two other lines should be modified (lines 6 and 7, in year 1). The results of applying the proposed wildfire-resilient planning algorithm in this case are displayed in Fig. 3. In Fig. 3a, it is noticed that up to year 6, all of the expected demand is served. However, in the last 4 years, some energy has not been served. The total amount of expected energy not served (EENS) for this network is equal to 41.2 GWh throughout the planning horizon. The overall demand in each year based on the realized uncertainties is also shown in this figure. Due to the uncertainties that are realized, the demand values do not demonstrate a strictly growing pattern. The non-zero value of EENS in year 7 in Fig. 3a is explained by the fluctuation of DER energy availability (parameter $\overline{p}^R$) at each year. On average, $\overline{p}^R$ in year 7 is 15% less than that in year 8. That is why it is observed that, unlike in year 7, the EENS in year 8 has reached zero, even though the demand value ($\overline{p}^D$) in this year has grown and the overall installed DER capacity has remained the same.

According to Fig. 3b, line de-energization enables the network to reduce the wildfire risk. The dark-colored bars in this figure show the network's overall wildfire risk if all of the lines remain connected. The light-colored bars represent the wildfire risk under the proposed scheme. The reduction in the wildfire risk under operating conditions is exclusively achieved through optimal line de-energization as the wildfire risk is determined by line energization status. Compared with the system's default configuration, where all of the lines remain energized, the wildfire-resilient planning decreases the overall wildfire risk by 77.5%. Compared with a scenario

TABLE III
EFFECT OF UNCERTAINTIES IN PLANNING DECISIONS AND COSTS

	With modeling uncertainties	Without modeling uncertainties
Number of new lines	2	1
Number of modified lines	2	1
Installed DER capacity (GW)	1,074.0	524.0
Dispatch of DER units (TWh)	29.4	16.8
Dispatch of Thermal units (TWh)	13.2	24.5
Wildfire risk	0.187	0.196
Load shedding (%)	0.10	2.97
VOLL ($M)	82.5	2,530.8
Planning costs ($M)	1,442.0	667.1
Overall system costs ($M)	1,771.3	3,656.1

TABLE IV
EFFECT OF RISK TOLERANCE IN PLANNING DECISIONS AND COSTS

	With limiting wildfire risk	Without limiting wildfire risk
Number of new lines	2	2
Number of modified lines	2	0
Installed DER capacity	1,074.0	1,047.9
Energized hours (%)	52.5	62.3
Wildfire risk	0.187	0.546
Load shedding (%)	0.10	0.09
Overall system costs ($M)	1,771.3	1,689.3

where no expansion investments are made and the decision-maker relies solely on PSPSs to limit wildfire risk, the overall wildfire risk remains almost equal to that of the wildfire-resilient expansion strategy. Compared with the PSPS scenario where a considerable amount of 25.29% of the load is shed, the proposed model will decrease load-shedding by more than 99%. Additionally, compared to the overall operating costs of the system which are equal to $20,222.4M in the PSPS case, the costs in the proposed expansion planning framework are reduced by more than 91%.

DER installation reduces the wildfire risk since they are mainly placed at demand buses and do not enforce line energization. It is noticed in Fig. 3c that DER units are the main energy providers of this network. According to Fig. 3d, 899.6 MW of DER capacity is installed in the first year, which is gradually increased to 1074.0 MW by the last planning year to meet the growing demand. The lowest amount of DER capacity is installed on Bus 2 (187.5 MW), which is not a demand bus.

1) The Importance of Modeling Uncertainties in the Expansion Planning Under Wildfire Risk: Proper modeling of the uncertainties contributes significantly to the effectiveness of the proposed resilient expansion planning scheme. While ignoring the uncertainties would decrease the expansion planning cost, it would end up with a much higher operation cost due to the significant increase in the VOLL. Table III summarizes the decisions for planning with and without preparing for uncertainties in the planning phase. It is observed that preparing for uncertainties incurs $764.9M higher planning costs in the construction of new lines, modification of the existing lines, and installation of DER units compared to the scenario where the planner is not ready for uncertain events. However, the realization of uncertainties leads to a $1,884.8M increase in system costs in the latter case, mainly due to the considerable difference of $2,448.3M in VOLL. In the former case, only 0.1% of the load is missed, while in the latter case, up to 2.97% of demand is shed. In our experiments, κ^D is considered equal to 2,000 $/MWh.

2) The Impact of Considering Wildfire Risk Levels in the Expansion Planning Problem: While a high level of wildfire risk could result in disastrous damages with costs beyond limits, modeling the risk within the expansion planning problem will significantly reduce it with a relatively small investment. Here, another scenario is investigated where the decision-maker does not pay attention to wildfire risk during the planning stage. This scenario could be modeled by assigning a high value to Υ in the constraint (1m) of the proposed expansion planning model. Table IV displays the results of two approaches where risk tolerance is limited and is not. The energized hours row denotes the percentage of the hours throughout the planning horizon that all of the lines have been switched on. Comparing the expansion planning results between cases where wildfire risk is limited and not limited, the overall system operation costs are only $82M higher in the former case. This is mainly because, in the latter case, no lines are modified and a smaller DER capacity is installed. However, the overall wildfire risk in the latter case is almost three times that in the former case. This observation suggests that with relatively small investments (4.9%) and careful operation (reflected by energized hours row), this network could achieve a substantially higher degree of resilience in operation against the risk of wildfire.

B. Exploring the Planner's Decision-Making Process and Risk Burden

A key parameter of Alg. 1 is the value of Υ, which essentially represents the amount of risk the planner is willing to take. A 'risk-averse' planner would opt for exceedingly small risk tolerance values, while a 'risk-seeker' planner wants to avoid proactive line de-energization and serve more demand with tolerating riskier situations. The latter behavior requires minimal investment costs and results in negligible load shedding, whereas the former behavior entails higher investments and considerable shut-off periods. Several other factors, including but not limited to network characteristics (size, population, infrastructure, instruments), policies, regional characteristics (climate, vegetation, historical wildfires, wildfire spread model), decision-maker's expertise, and risk-taking inclination also impact the choice of Υ. Here, several scenarios with different levels of Υ are simulated to investigate the impact of risk tolerance on the wildfire-resilient planning problem. Since the choice of Υ is somewhat a subjective matter, we have presented results for planners with different risk-taking inclinations. The system planner may consider various value for their risk and assess based on the balance between VOLL and network expansion cost.

It is noticed that the choice of wildfire risk tolerance heavily affects the network's planning costs. According to the results displayed in Table V, generally with lower tolerance levels,

TABLE V
PLANNING DECISIONS IN CASE OF RISK TOLERANCE ANALYSIS

Risk-taking inclination	Υ	Number of new lines	Number of modified lines	Installed DER (MW)	Overall costs ($M)
Risk-seeker	0.080	2	0	1090	1,759.7
Risk-neutral	0.020	2	2	1,073	1,771.3
Risk-averse	0.010	2	6	1,144	3,270.1
Risk-averse	0.005	2	4	1,248	8,303.8

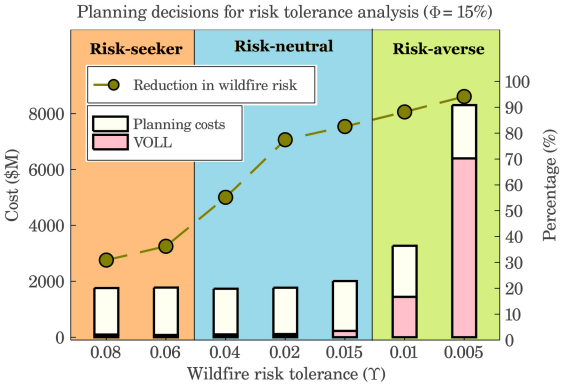

Fig. 4. Network cost and risk reduction in case of risk tolerance analysis.

more lines are required to be modified and higher DER capacity is installed. Since the wildfire risk of new lines is zero (it is considered that the new lines are underground), the addition of new lines does not increase the wildfire risk. Additionally, new line construction could allow for the switching off of some of the existing transmission lines, which consequently reduces the wildfire risk. With lower risk tolerance levels, more lines are generally modified. An exception is the last instance ($\Upsilon = 0.005$) in which, by reducing the wildfire risk tolerance level, the number of modified lines is reduced. It is noticed that in this instance, the amount of installed DER capacity has increased compared to its previous instance ($\Upsilon = 0.010$). Since DERs installed in these two instances are strictly located at the demand buses, the addition of more DER capacity translates into less energization of lines, which inhibits the wildfire ignition risk. It is noticed that planners are categorized into three groups based on their inclination to take risks. The authors have grouped the planners based on the percentage of lost load, where this value is less than 0.1% for a risk-seeker planner, higher than 1% for a risk-averse planner, and anything in between for a risk-neutral planner.

The network's overall wildfire risk can be managed through higher investments. However, this is not always the case, and to match lower tolerance levels, some parts of the network must be de-energized. The cost analysis results displayed in Fig. 4 suggests that with the reduction in risk tolerance, the overall system costs increase mostly due to the increase in VOLL. It is noticed that with lower degrees of risk tolerance, the overall planning costs of the system (costs of new line construction, line modification, DER installation, and generation of thermal units) do not experience a considerable increase (from $1,663.9M in the first instance to $1,905.3M in the last instance). This observation suggests that expansion planning

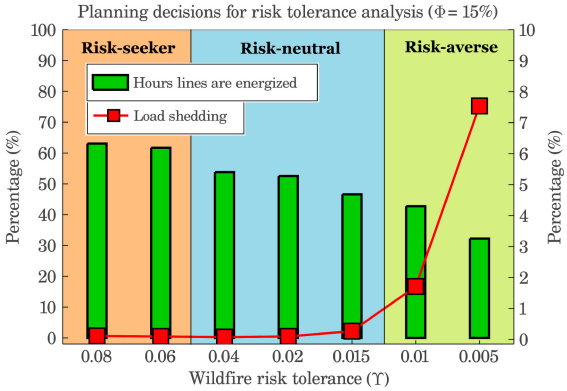

Fig. 5. Load shedding and line energization in case of risk tolerance analysis.

investments are not enough to obtain lower risk tolerance levels. It is observed that for risk-averse planners, VOLL has a substantial share in the overall system costs. After a certain point, the system decision-maker should start shutting off power to the consumers to match the reduced risk tolerance. The dashed line (right axis) in Fig. 4 displays the reduction in the overall system wildfire risk score in percentage for each tolerance level. This value is obtained by comparing the actual wildfire risk of the system with the total wildfire risk if all lines are switched on. It is noticed that in the case where risk tolerance is 0.08, the network's wildfire risk is reduced by 30.9%, whereas in the case where only 0.005 wildfire risk is tolerated, the overall risk is reduced by 97.2%.

To match the decreasing risk tolerance value, fewer lines are being energized and more load is being shed. According to the analysis results displayed in Fig. 5, it is observed that in the case where risk tolerance equals 0.08, 63.1% of the lines are energized at all times. It is noticed if the risk tolerance is reduced to 0.005, the hours lines are energized are almost halved (32.2%). This reduction is mainly because network expansion decisions are limited in their ability to maintain a lower risk level. The right axis shows the percentage of load shedding in each instance. It is noticed that the reduction in risk tolerance comes at the price of higher EENS. The load shedding percentage increases from less than 0.1% in the first instance to a considerable amount of 7.5% in the last instance.

C. The Side Benefits of Transmission Switching

In this part, it is illustrated how transmission switching is beneficial to wildfire-resilient expansion planning by reducing wildfire risk and EENS. In the previous case, it was noticed in Fig. 5 that the percentage of energized lines decreases with the reduction in risk tolerance levels. According to Eqs. (1l) and (1m), risk tolerance is calculated based on energized lines. So it is only natural that in cases where line addition or modification is not enough to reduce the network's overall risk, fewer lines become energized. This argument suggests that if the overall risk of the network when all of the lines are switched on is less than the wildfire tolerance level, no more line de-energization is necessary. For example, it was noticed in Table IV that even when the tolerance limit is not enforced, the lines are de-energized 37.8% of the time. This observation

TABLE VI
RESULTS OF TRANSMISSION SWITCHING ANALYSIS

Case	*With* switching	*Without* switching
Number of new lines	2	2
Number of modified lines	0	4
Installed DER capacity (MW)	1,090.0	1,290.3
Dispatch of DER units (TWh)	30.5	30.6
EENS (GWh)	47.9	48.9
Energized hours (%)	63.1	100
Overall system costs ($M)	1,759.7	2,033.1

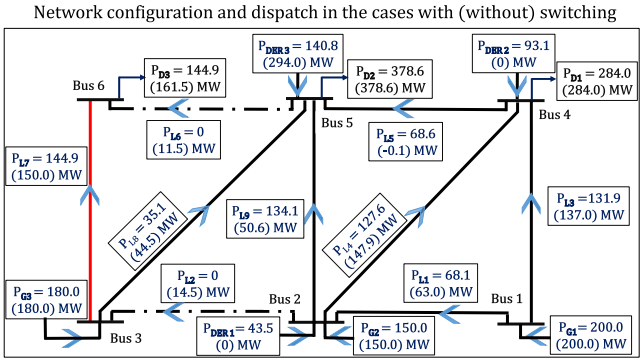

Fig. 6. Comparison of network configuration in two cases during period 6 at year 10.

suggests that line switching is taking place for a reason other than wildfire risk reduction.

In this part, the effects of transmission switching on the operation of the 6-bus network presented in Case A are investigated. Two cases are considered: 1- *With* switching, in which line switching decisions are allowed and determined by the optimization problem. 2- *Without* switching, in which all of the lines are forced to stay energized at all periods. The results of these two cases are compared against each other in Table VI. The second and the third columns in Table VI respectively correspond with the case where lines are able to be switched on/off (*with* switching) and the case where lines are forcefully switched on (*without* switching). In these experiments, Φ is set to 15% while Υ is considered equal to 0.08.

It is noticed that transmission switching reduces the network's overall costs. This is mainly due to the requirement for modification of lines and installation of larger DER capacity in the case *without* switching. Additionally, it is observed that in the case *with* transmission switching, the percentage of hours lines are energized is reduced to 63.1% which decreases the overall wildfire risk.

Transmission switching takes place in a way that limits congestion for each period. The on/off switching decisions at each duration result in different network configurations and dispatch. The configuration of the 6-bus network during period 3 for cases *with* switching and *without* switching is shown in Fig. 6, where dispatch values for the latter case are displayed inside brackets. According to these results, it is only during period 3 (which corresponds with the peak demand in the load duration curve) that the system is not able to meet all of the demand. In the case where switching is allowed, lines 2 and 6 are switched off to facilitate load delivery. As a result, the served demand in the case *with* switching is 16.6 MW more than that of the case *without* switching. In the case of *without* switching, line 7 reaches its maximum power flow limit and is distinguished by its red color.

It should be noted that in current real-world PSPS practices, sectionalizing high-risk areas from the rest of the network is an inefficient process. The boundary of the regions that lose service during PSPS events is determined by the availability of proper switching devices. That is why Californian utilities such as San Diego Gas & Electric have intensively engaged in sectionalizing enhancement programs by installing new isolation switches [17].

TABLE VII
PLANNING DECISIONS IN CASE OF BOU ANALYSIS

Φ (%)	Number of new lines	Number of modified lines	Installed DER capacity (MW)	Overall planning costs ($M)
0	1	1	524.0	1,123.8
5	1	1	895.0	1,537.4
10	2	1	989.7	1,646.2
15	2	2	1074.0	1,771.3
20	2	2	1156.3	1,862.0
25	2	2	1152.3	1,883.0

D. Implications of Uncertainties on Expansion Planning Decisions

In this case, various scenarios for the wildfire-resilient planning of the 6-bus network are presented to investigate the impact of uncertainties on expansion planning decisions. Another control parameter in Algorithm 1 is the value of Φ. To explore the impacts of this choice, several simulations were performed with different BoU levels. Similar to the choice of risk tolerance, the system planner can choose the BoU based on its preferences or the network's conditions. According to the expansion planning results displayed in Table VII, it is observed that higher uncertainty levels require more investments in new line construction, line modification, and DER installations. In these simulations, the risk tolerance value (Υ) is set to 0.02 and the 6-bus network presented in Case A is considered.

By increasing the BoU, the output of DERs is more likely to be reduced. That is why higher BoU levels require increased DER capacity to hedge against uncertainties. According to the cost breakdown results displayed in Fig. 7, the installation cost of DER units accounts for the largest share of the overall system costs. It is noticed that with an increase in the uncertainty level, the cost of expansion, generation, and VOLL do not experience considerable growth.

It is also observed that demand uncertainties are more likely to lead to undesirable scenarios. Fig. 8 displays how many instances of realized uncertainties are allocated to demand and DERs at each instance. It is observed that worst-case realizations correspond with the larger portion of uncertainties happening in demand. As a result, the overall system demand is increasing due to the growth in uncertainty levels. However, it is also observed that at $\Phi = 25\%$, the share of demand and DERs in realized uncertainties is almost equal. This observation suggests that the drop in DER outputs could aggravate

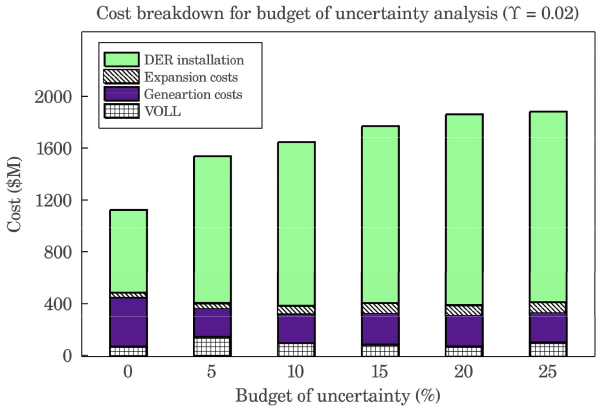

Fig. 7. Breakdown of system costs for BoU analysis.

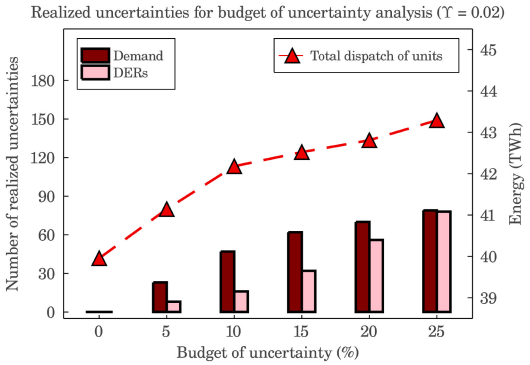

Fig. 8. Uncertainties realized and total dispatch of units for BoU analysis.

system operations as much as an increase in demand. The right axis of Fig. 8 shows the total amount of energy dispatched for different BoU levels. As expected, it is noticed that a higher BoU requires increased dispatched energy.

E. A Scenario With Higher Number of Potential New Lines

A larger set of candidate new lines results in lower expansion costs. In the experiments performed on the 6-bus network, it was assumed that the set of new lines consists of only two lines, i.e., lines 8 and 9. Here, another scenario is explored where the set of new lines is increased to four lines. It is assumed that two other potential new lines are added to set $\mathcal{N}$, with candidate lines 10 and 11 connecting bus pairs 2-6 and 1-5, respectively. The results of applying the wildfire-resilient planning strategy to the same 6-bus network with different sets of candidate new lines suggest the choice of candidate line heavily impacts the expansion decisions and costs. According to Table VIII, in the case where 2 candidate lines are assigned, some lines should be modified with lower risk tolerance levels, whereas in the case with 4 candidate lines, no lines are modified. In the former case, lines 8 and 9 are constructed in all instances, while in the latter case, lines 8 and 10 are added. It is noticed that in the last instance, the larger set of candidate lines leads to a 48% reduction in planning costs (which is interestingly achieved only by building line 10 instead of line 9). However, transmission line routing is a challenging issue that limits the practicality of this approach.

TABLE VIII
COMPARISON OF EXPANSION PLANNING DECISIONS AND COSTS FOR DIFFERENT SETS OF CANDIDATE LINES

ϒ	$\mathcal{N} = \{L8, L9\}$			$\mathcal{N} = \{L8, L9, L10, L11\}$		
	Number of new lines	Number of modified lines	Cost ($M)	Number of new lines	Number of modified lines	Cost ($M)
0.040	2 (L8, L9)	0	1,733.9	2 (L8, L10)	0	1,621.9
0.020	2 (L8, L9)	2	1,771.3	2 (L8, L10)	0	1,626.2
0.010	2 (L8, L9)	6	3,270.1	2 (L8, L10)	0	1,686.0

TABLE IX
EXPANSION PLANNING RESULTS IN 118-BUS CASE ($\Upsilon = 0.1$, $\Phi = 10\%$)

Number of new lines	6
Number of modified lines	1
Installed DER capacity (MW)	3,856.1
Dispatch of DER units (TWh)	105.6
Dispatch of thermal units (TWh)	51.3
DER installation cost ($M)	4,674.5
Generation cost ($M)	1,503.9
Overall system costs ($M)	6,340.8
Load shedding (%)	0.04
Wildfire risk reduction	64.9 %

F. IEEE 118-Bus Power System

In this part, a sub-region in the IEEE 118-bus network including 43 existing lines and 14 candidate new lines is considered. It is assumed that all of the existing lines considered in the wildfire-resilient expansion planning are equipped with switches and can be modified. The results suggest that similar to previous cases, the expansion planning costs are dominated by DER installation expenses, while with relatively low investment in the addition and modification of lines, the overall network wildfire risk is reduced by 65%. The expansion decisions obtained by the proposed wildfire-resilient algorithm are reported in Table IX. It is noticed that the thermal units account for only one-third of the total dispatched energy, while the rest of the demand is served by DER units. The percentage of load shedding is minimal in this case, which means achieving a risk tolerance level of 0.1 is not challenging for this system.

V. CONCLUSION

In this paper, an expansion planning model is presented to limit the wildfire ignition risk of electricity networks and model the long-term impacts of public safety power shut-off events. The results illustrate how decision-makers can strike a balance between shutting off power to customers and grid expansion or hardening measures. The results demonstrate that DER installation is the best approach to meet demand growth and inhibit wildfire risk in the long run. Our simulations suggest that transmission line switching plays a major role in keeping the overall wildfire risk of the network below the tolerance level and facilitating demand serving. Lowering wildfire risk tolerance and raising the level of uncertainty will require more investment costs. However, new line construction, line modification, and DER installations can not always guarantee network operation within desired wildfire-safe risk levels.

It is shown that, at some point, de-energizing lines and shutting off customers is inevitable to maintain a wildfire-resilient operation.

REFERENCES

[1] K. T. Weber and R. Yadav, "Spatiotemporal trends in wildfires across the western United States (1950–2019)," *Remote Sens.*, vol. 12, no. 18, p. 2959, 2020.

[2] W. M. Jolly et al., "Climate-induced variations in global wildfire danger from 1979 to 2013," *Nat. Commun.*, vol. 6, no. 1, pp. 1–11, 2015.

[3] "Pacific gas and electric company amended 2019 wildfire safety plan," Pacific Gas Elect. Company, San Francisco, CA, USA, 2019. Accessed: Oct. 2021. [Online]. Available: https://bit.ly/3xpYvzI

[4] Texas wildfire mitigation project. "How do power lines cause wildfires?" 2014. [Online]. Available: https://bit.ly/3b1kT7b

[5] J. E. Keeley and A. D. Syphard, "Historical patterns of wildfire ignition sources in California ecosystems," *Int. J. Wildland Fire*, vol. 27, no. 12, pp. 781–799, 2018.

[6] "Utility company PSPS post event reports." California Public Utilities Commission, San Francisco, CA, USA, 2020. Accessed: Oct. 2021. [Online]. Available: https://bit.ly/3pGyqdu

[7] A. D. Syphard and J. E. Keeley, "Location, timing and extent of wildfire vary by cause of ignition," *Int. J. Wildland Fire*, vol. 24, no. 1, pp. 37–47, 2015.

[8] J. W. Mitchell, "Power line failures and catastrophic wildfires under extreme weather conditions," *Eng. Fail. Anal.*, vol. 35, pp. 726–735, Dec. 2013.

[9] A. Arab, A. Khodaei, R. Eskandarpour, M. P. Thompson, and Y. Wei, "Three lines of defense for wildfire risk management in electric power grids: A review," *IEEE Access*, vol. 9, pp. 61577–61593, 2021.

[10] W. Jahn, J. L. Urban, and G. Rein, "Powerlines and Wildfires: Overview, perspectives, and climate change: Could there be more electricity blackouts in the future?" *IEEE Power Energy Mag.*, vol. 20, no. 1, pp. 16–27, Jan./Feb. 2022.

[11] R. Serrano et al., "Fighting against wildfires in power systems: Lessons and resilient practices from the Chilean and Brazilian experiences," *IEEE Power Energy Mag.*, vol. 20, no. 1, pp. 38–51, Jan./Feb. 2022.

[12] P. Murphy, "Preventing wildfires with power outages: The growing impacts of California's public safety power Shutoffs," PSE Healthy Energy, Oakland, CA, USA, 2021. Accessed: Oct. 2021. [Online]. Available: https://bit.ly/3CponkD

[13] M. Sotolongo, C. Bolon, and S. H. Baker, "California power Shutoffs: Deficiencies in data and reporting," 2020. Accessed: Oct. 2021. [Online]. Available: https://bit.ly/3wfPibX

[14] P. Stevens, "PG&E power outage could cost the California economy more than $2 billion," CNBC, Englewood Cliffs, NJ, USA, 2019. Accessed: Oct. 2021. [Online]. Available: https://cnb.cx/36e21kR

[15] R. Bayani, M. Waseem, S. D. Manshadi, and H. Davani, "Quantifying the risk of wildfire ignition by power lines under extreme weather conditions," *IEEE Syst. J.*, early access, Jul. 26, 2022, doi: 10.1109/JSYST.2022.3188300.

[16] "Powerline bushfire safety program-vegetation conduction ignition test report and data," Dept. Environ., Land, Water & Planning, East Melbourne, VIC, Australia, 2016. Accessed: Aug. 2022. [Online]. Available: https://bit.ly/3TRU4cs

[17] E. A. Udren, C. Bolton, D. Dietmeyer, T. Rahman, and S. Flores-Castro, "Managing wildfire risks: Protection system technical developments combined with operational advances to improve public safety," *IEEE Power Energy Mag.*, vol. 20, no. 1, pp. 64–77, Jan./Feb. 2022.

[18] B. Chiu, R. Roy, and T. Tran, "Wildfire resiliency: California case for change," *IEEE Power Energy Mag.*, vol. 20, no. 1, pp. 28–37, Jan./Feb. 2022.

[19] C. Ruiz and A. J. Conejo, "Robust transmission expansion planning," *Eur. J. Oper. Res.*, vol. 242, no. 2, pp. 390–401, 2015.

[20] N. Amjady, A. Attarha, S. Dehghan, and A. J. Conejo, "Adaptive robust expansion planning for a distribution network with DERs," *IEEE Trans. Power Syst.*, vol. 33, no. 2, pp. 1698–1715, Mar. 2018.

[21] M. Farhoumandi, F. Aminifar, and M. Shahidehpour, "Generation expansion planning considering the rehabilitation of aging generating units," *IEEE Trans. Smart Grid*, vol. 11, no. 4, pp. 3384–3393, Jul. 2020.

[22] S. D. Manshadi and M. E. Khodayar, "Expansion of autonomous microgrids in active distribution networks," *IEEE Trans. Smart Grid*, vol. 9, no. 3, pp. 1878–1888, May 2018.

[23] D. Pozo, E. E. Sauma, and J. Contreras, "A three-level static MILP model for generation and transmission expansion planning," *IEEE Trans. Power Syst.*, vol. 28, no. 1, pp. 202–210, Feb. 2013.

[24] A. Moreira, D. Pozo, A. Street, and E. Sauma, "Reliable renewable generation and transmission expansion planning: Co-optimizing system's resources for meeting renewable targets," *IEEE Trans. Power Syst.*, vol. 32, no. 4, pp. 3246–3257, Jul. 2017.

[25] S. Li, D. W. Coit, and F. Felder, "Stochastic optimization for electric power generation expansion planning with discrete climate change scenarios," *Elect. Power Syst. Res.*, vol. 140, pp. 401–412, Nov. 2016.

[26] J. K. Skolfield, A. R. Escobedo, and J. RamirezVergara, "Transmission and capacity expansion planning against rising temperatures: A case study in Arizona," in *Proc. IISE Annu. Conf. Expo*, 2021, pp. 872–877.

[27] A. Flores-Quiroz, R. Palma-Behnke, G. Zakeri, and R. Moreno, "A column generation approach for solving generation expansion planning problems with high renewable energy penetration," *Elect. Power Syst. Res.*, vol. 136, pp. 232–241, Jul. 2016.

[28] B. Chen, J. Wang, L. Wang, Y. He, and Z. Wang, "Robust optimization for transmission expansion planning: Minimax cost vs. minimax regret," *IEEE Trans. Power Syst.*, vol. 29, no. 6, pp. 3069–3077, Nov. 2014.

[29] J. Li et al., "Robust coordinated transmission and generation expansion planning considering ramping requirements and construction periods," *IEEE Trans. Power Syst.*, vol. 33, no. 1, pp. 268–280, Jan. 2018.

[30] H. Yu, C. Chung, K. Wong, and J. Zhang, "A chance constrained transmission network expansion planning method with consideration of load and wind farm uncertainties," *IEEE Trans. Power Syst.*, vol. 24, no. 3, pp. 1568–1576, Aug. 2009.

[31] B. Zeng and L. Zhao, "Solving two-stage robust optimization problems using a column-and-constraint generation method," *Oper. Res. Lett.*, vol. 41, no. 5, pp. 457–461, 2013.

[32] D. Bertsimas, E. Litvinov, X. A. Sun, J. Zhao, and T. Zheng, "Adaptive robust optimization for the security constrained unit commitment problem," *IEEE Trans. Power Syst.*, vol. 28, no. 1, pp. 52–63, Feb. 2013.

[33] G. Byeon, P. Van Hentenryck, R. Bent, and H. Nagarajan, "Communication-constrained expansion planning for resilient distribution systems," *INFORMS J. Comput.*, vol. 32, no. 4, pp. 968–985, 2020.

[34] H. Nagarajan, E. Yamangil, R. Bent, P. Van Hentenryck, and S. Backhaus, "Optimal resilient transmission grid design," in *Proc. Power Syst. Comput. Conf. (PSCC)*, 2016, pp. 1–7.

[35] C. Shao, M. Shahidehpour, X. Wang, X. Wang, and B. Wang, "Integrated planning of electricity and natural gas transportation systems for enhancing the power grid resilience," *IEEE Trans. Power Syst.*, vol. 32, no. 6, pp. 4418–4429, Nov. 2017.

[36] B. Zou, C. Wang, Y. Zhou, J. Wang, C. Chen, and F. Wen, "Resilient co-expansion planning between gas and electric distribution networks against natural disasters," *IET Gener. Transm. Distrib.*, vol. 14, no. 17, pp. 3561–3570, 2020.

[37] H. Hamidpour, S. Pirouzi, S. Safaee, M. Norouzi, and M. Lehtonen, "Multi-objective resilient-constrained generation and transmission expansion planning against natural disasters," *Int. J. Elect. Power Energy Syst.*, vol. 132, p. 13, Nov. 2021.

[38] D. N. Trakas and N. D. Hatziargyriou, "Optimal distribution system operation for enhancing resilience against wildfires," *IEEE Trans. Power Syst.*, vol. 33, no. 2, pp. 2260–2271, Mar. 2018.

[39] T. Tapia, Á. Lorca, D. Olivares, M. Negrete-Pincetic, and A. J. Lamadrid L, "A robust decision-support method based on optimization and simulation for wildfire resilience in highly renewable power systems," *Eur. J. Oper. Res.*, vol. 294, pp. 723–733, Oct. 2021.

[40] D. L. Donaldson, M. S. Alvarez-Alvarado, and D. Jayaweera, "Power system resiliency during wildfires under increasing penetration of electric vehicles," in *Proc. Int. Conf. Probabil. Methods Appl. Power Syst. (PMAPS)*, 2020, pp. 1–6.

[41] J. W. Muhs, M. Parvania, and M. Shahidehpour, "Wildfire risk mitigation: A paradigm shift in power systems planning and operation," *IEEE Open Access J. Power Energy*, vol. 7, pp. 366–375, 2020.

[42] "Transmission initiative routing study: An initiative to export Nevada's renewable energy," Nevada Governor's Office Energy, Carson City, NV, USA, 2012. Accessed: Oct. 2021. [Online]. Available: https://energy.nv.gov/Media/Reports/

Reza Bayani (Graduate Student Member, IEEE) received the B.Sc. degree in electrical engineering from the Sharif University of Technology, Tehran, Iran, in 2013, and the M.Sc. degree in electrical engineering from the Iran University of Science and Technology, Tehran, Iran, in 2016. He is currently pursuing the Ph.D. degree in electrical and computer engineering with the University of California at San Diego, La Jolla, CA, USA, and San Diego State University, San Diego, CA, USA. His current research interests include power system operation and planning, machine learning, and transportation electrification. He is a Ph.D. Fellow of California State University's Chancellor's Doctoral Incentive Program and was awarded SDSU's 2022–2023 University Graduate Fellowship.

Saeed D. Manshadi (Member, IEEE) received the B.S. degree in electrical engineering from the University of Tehran, Tehran, Iran, the M.S. degree from the University at Buffalo, the State University of New York, Buffalo, NY, USA, and the Ph.D. degree from Southern Methodist University, Dallas, TX, USA. He is an Assistant Professor with the Department of Electrical and Computer Engineering, San Diego State University. He was a Postdoctoral Fellow with the Department of Electrical and Computer Engineering, University of California at Riverside, Riverside. His current research interests include smart grid, transportation electrification, microgrids, integrating renewable and distributed resources, and power system operation and planning. He serves as an Editor for IEEE TRANSACTIONS ON VEHICULAR TECHNOLOGY.